

# Cancellation of probe effects in measurements of spin polarized momentum density by electron positron annihilation.

M. Biasini<sup>1, #</sup>, J. Ruzs<sup>3</sup>

<sup>1</sup> Department of Physics, University of California at Riverside, Riverside, California 92521, USA

<sup>2</sup> Department of Electronic Structures, Charles University, Ke Karlovu 5, 12116 Prague 2, Czech Republic

(Dated: June 15, 2018)

Measurements of the two dimensional angular correlation of the electron-positron annihilation radiation have been done in the past to detect the momentum spin density and the Fermi surface. We point out that the momentum spin density and the Fermi Surface of ferromagnetic metals can be revealed within great detail owing to the large cancellation of the electron-positron matrix elements which in paramagnetic multiatomic systems plague the interpretation of the experiments. We prove our conjecture by calculating the momentum spin density and the Fermi surface of the half metal CrO<sub>2</sub>, who has received large attention due to its possible applications as spintronics material.

PACS numbers: 71.18.+y, 71.27.+a, 71.60.+z, 78.70.Bj

Keywords: density functional theory, positron annihilation, 2D-ACAR, CrO<sub>2</sub>, Fermi surface

To a great extent, the Fermi surface (FS) can be regarded as the defining property of a metal. It is an ubiquitous concept which appears in numberless works devoted to the study of the electronic structure of systems which, under some particular circumstance, seem to show metallic behaviour. In several cases, the initial task of establishing metallic behavior is not easy since different probes can yield contrasting answers. Clearly, an experimental investigation of the FS implies the observability of the electrons sitting in the *partially filled* energy bands, which, in turn, requires interaction of the conduction electron with the experimental probe.

In the case of a measurement of the two dimensional angular correlation of electron positron annihilation radiation (2D-ACAR), the FS is revealed through discontinuities (breaks) in the electron positron momentum density,  $\rho^{ep}(\mathbf{p})$  [1] at points  $\mathbf{p}_{F_i} = (\mathbf{k}_{F_i} + \mathbf{G})$ , where  $\mathbf{G}$  is a reciprocal lattice vector and  $\mathbf{k}_{F_i}$  are the reduced Fermi wave vectors in the first BZ. While the locations of the FS breaks are faithfully preserved [2], the resulting single particle electron momentum density,  $\rho^e(\mathbf{p})$ , is severely modulated by the non uniform positron (spatial) density and the electron-positron Coulomb interaction. In this letter we show that in the special case of a ferromagnetic sample, the probe modulation is strongly suppressed, allowing a faithful representation of the spin polarized momentum density and unambiguous interpretation of the data. The FS breaks are reinforced by the Lock-Crisp-West (LCW) transformation [3], consisting of folding the momentum distribution  $\rho^{ep}(\mathbf{p})$  back onto the first BZ by translation over the appropriate vectors  $\mathbf{G}$ . The result of the summation (denoted as LCW density) is [4],

$$\rho_{LCW}^{ep}(\mathbf{k}) = \sum_n \theta(E_F - \epsilon_{\mathbf{k},n}) \int |\psi_{\mathbf{k}}^n(\mathbf{r})|^2 |\phi(\mathbf{r})|^2 g(\mathbf{r}) d\mathbf{r}. \quad (1)$$

Here  $\psi_{\mathbf{k}}^n$  and  $\phi$  denote the electron and positron wave function, respectively,  $E_F$  is the Fermi level and  $\epsilon_{\mathbf{k},n}$  is

the energy eigenvalue of the electron from band  $n$  with Bloch wavevector  $\mathbf{k}$ . The enhancement factor [5]  $g(\mathbf{r})$ , describes the enhancement of the electronic density at the positron location due to the Coulomb force. If the  $\mathbf{k}, n$  dependence of the overlap integral in eq. 1 is negligible,  $\rho_{LCW}^{ep}(\mathbf{k})$  is reduced to the *occupancy*, i.e. the number of occupied bands per  $\mathbf{k}$  point. The FS manifolds are the loci of the breaks of the occupancy. A significant drawback of 2D-ACAR is that all the outer electrons overlap (to some extent) with the positron probe. Therefore, when the orbital character of one full valence band changes noticeably in the BZ, the related LCW density acquires a  $\mathbf{k}$ -dependence which is superimposed to the changes in the occupancy due to the FS breaks of the conduction bands. For example, our recent work on UGa<sub>3</sub> [6] has detected a noticeable change in the  $p$  character of three valence bands located 1-2 eV below  $E_F$  which did obscure greatly the visibility of the FS. Further notable examples are high-Tc superconductors where strong positron wave function effects prevented the observation of the critical FS sheets linked to the Cu-Oxide planes, which are responsible of superconductivity [7, 8].

Obviously, the elimination of the contribution of all the filled bands from the LCW summation would increase greatly the visibility of the FS whenever the overlap integral of eq. 1 is  $\mathbf{k}$ (valence)-dependent. This favorable situation is indeed realized in the measurement of the spin polarized bands of ferromagnetic metals. In this case, the employment of 2D-ACAR experiments [9, 10, 11] hinges on two facts: i) the intrinsic polarization  $P_{e^+}$  for positrons produced during  $\beta$  decay (for the <sup>22</sup>Na source  $P_{e^+}$ , averaged over angle and velocity, is about 36%). ii) the annihilation selection rule which requires that the positron may undergo  $2\gamma$  annihilation only if the spins of the annihilating pair form a singlet state.

Therefore, by performing 2D-ACAR measurements with the magnetic substance polarized (by an external magnetic field) in directions respectively parallel and an-

tiparallel to the average positron polarization (which is unchanged upon reversal of the magnetic field) will then yield an observable imbalance of  $2\gamma$  annihilations with respect to the majority or minority spins. The experimental spectra taken when the positron polarization is parallel (antiparallel) to the polarizing magnetic field will be

$$\begin{aligned} \rho_{par,antipar}^{ep}(\mathbf{p}) = & 1/2(1 \pm P_{e^+})[N^M(\mathbf{p}) + N^{NM}(\mathbf{p})/2] + \\ & + 1/2(1 \mp P_{e^+})[N^m(\mathbf{p}) + N^{NM}(\mathbf{p})/2], \end{aligned} \quad (2)$$

where  $N^{NM}$  refers to the contribution from the spin degenerate (i.e. non magnetic) bands. Subtraction of  $\rho_{par}^{ep}$  from  $\rho_{antipar}^{ep}$  yields the net momentum spin density  $\rho_{spin}^{ep}(\mathbf{p})$ .

$$\rho_{spin}^{ep}(\mathbf{p}) = P_{e^+}[\rho_{par}^{ep}(\mathbf{p}) - \rho_{antipar}^{ep}(\mathbf{p})]. \quad (3)$$

Equations 2 and 3 are equally applicable to the electron positron momentum density,  $\rho^{ep}(\mathbf{p})$ , or to the LCW density, yielding for the latter case, the LCW net spin density  $\rho_{LCW\ spin}^{ep}(\mathbf{k})$ .

The main point of this work is the disappearance of  $N^{NM}$  and all the positron wave function effects related to the bands in question. As obvious as it may appear, this interesting result has, to our knowledge, never been pointed out and should prove to be very useful in future studies of ferromagnetic metals.

To investigate our conjecture we have chosen to examine  $\text{CrO}_2$  which is predicted to be a half metal by a variety of ab initio band structure calculations [12, 13, 14, 15]. Due to this result  $\text{CrO}_2$  has attracted much attention in the field of spintronics for its potential use as injector of a highly (nominally 100%) spin polarized current in the future *field effect spin transistor*. A puzzling result of the calculations is that different recipes to approximate the exchange correlation potential,  $U_{xc}$  (local spin density approximation (LSDA) [16] and Generalized Gradient Approximation (GGA) [17]) lead to unusually noticeable differences in the FS topology [13]. A further interesting result is that the standard LSDA and GGA seem to explain ultraviolet photoemission spectroscopy (UPES) experiments[18] better than the LDA+ $U$  method, [15], which usually is more suited to treat strong electron correlations.

In Refs. 6, 19 we have presented a method to calculate directly the LCW density via eq. 1. As a base for our calculation we used the scalar relativistic full-potential linearized augmented plane waves method (FP-LAPW) implemented in the WIEN2k package [20]. Compared to similar works of other authors [4, 21], our scheme, including electron-positron correlation effects [5], being *full potential* and compatible with any option of WIEN2k, which include spin-orbit (s.o.) interaction, LDA+ $U$  and orbital polarization, is more suited to the study of nar-

row bands and electron correlations.

The extension of the scheme to spin polarized calculations is relatively straightforward. The same steps used in the paramagnetic calculations are done for spin up and spin down electrons separately. In the absence of s.o. interaction the result consists of *pure* up spin and down spin bands. After the inclusion of s.o. each Bloch state becomes a combination of spin up and down components. For each band crossing  $E_F$  there is now an up and down spin submanifold, both having the same occupancy (and therefore the same Fermi surface). The amplitudes of these submanifolds are, however, different. Owing to parity and angular momentum conservation, the positron essentially *projects* the electronic states over the spin up or down manifolds.

The crystal structure of  $\text{CrO}_2$  is simple tetragonal (Rutile type, space group  $P4_2/mnm$ , [12]) with two formula units per unit cell. Details of the calculations, performed adopting  $U_{xc}$  according to GGA and LDA in the paramagnetic and ferromagnetic phases, are reported elsewhere [22]. The calculated majority spin bands are in excellent agreement with those reported by Mazin et al [13]. The main finding of the calculation is the half metallic behaviour, with a large energy gap ( $\simeq 2\text{eV}$ ) in the minority spin bands. The conduction bands have a very strong Cr  $d$  character, which is ascribed to states of  $t_{2g}$  symmetry. It is worth noting that the Cr-d orbital character of all the conduction bands is rather constant along each of the high symmetry directions.

As mentioned above, the topology of the holelike FS sheet, shown in Fig. 1(I,II)b depends noticeably on the kind of  $U_{xc}$  (LSDA,GGA). Whereas in the GGA case this

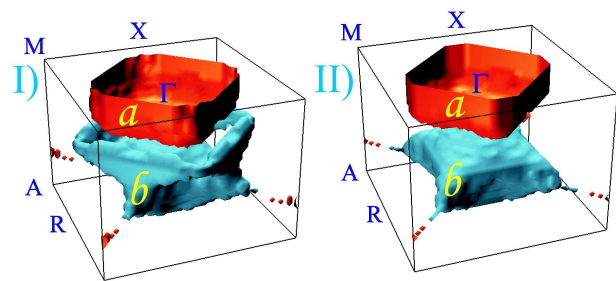


FIG. 1: The two FS sheets (a,b) of FM  $\text{CrO}_2$ , shown in half BZ (Online color: a:orange, electronlike; b:blue, holelike) produced with  $U_{xc}$  from LSDA (I) and GGA (II) [16, 17]. Here and in the next figures capital letters label the high symmetry points of the BZ.

FS has a simple, pillow-like shape (Fig. 1/II-b), the corresponding FS manifold resulting from LSDA (Fig. 1/I-b) is a pseudosphere connected to a toroidal structure with rhombic shape. On the other hand, the electronlike,  $\Gamma$  centred structure, yielded by the two calculations is very similar. Since  $\text{CrO}_2$  is a compensated metal (a necessary condition of any half metal), the electronlike and holelike

sheets have equal volume. The Fermi volumes resulting from LSDA and GGA differ slightly, corresponding to 12.8% of the BZ and 10.7% of the BZ for LSDA and GGA, respectively.

The predicted response of a 2D-ACAR experiment ex-

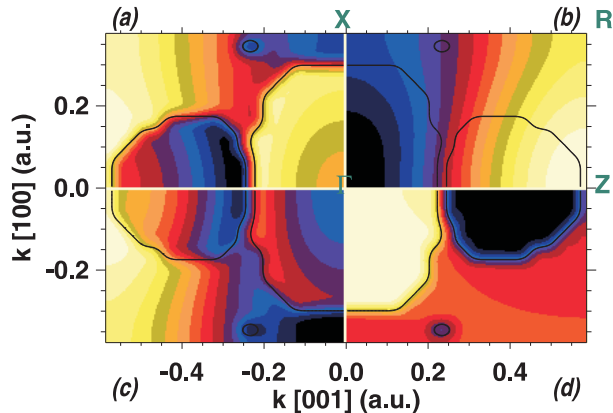


FIG. 2: (Online color.) FLAPW calculations for  $\text{CrO}_2$  in the (010) plane of the tetragonal BZ: (a) up spin LCW density; (b) down spin LCW density; (c) (a)+(b); (d) (a)-(b). The black contour denote the intersections of the two main FS sheets (see fig 1) with the (010) plane. Note that the horizontal direction is along [001]

periment can be elucidated by a slice of the calculated LCW density (adopting LSDA) in the (010) plane (GGA yields little difference in this plane; recall Fig 1). In Fig. 2 panels (a) and (b) refer to the majority and minority spins LCW densities, respectively, whereas panels (c) and (d) denote sum and difference of panels (a) and (b). These panels would be obtained by an experiment with 100% spin polarized positrons impinging a sample where the polarizing magnetic field is parallel or antiparallel to the positron polarization. In panel (a) the breaks pertaining to the electronlike and holelike FS sheets appear rather clearly (compare the changes of gray scale (or color) with the contour line marking the FS breaks), in spite of a strong modulation caused by a non uniform positron density. This modulation is the only feature appearing in panel (b), consistent with a negligible spin up-down mixing due to s.o. (WIEN2k yields 99.97% electron polarization at  $E_F$ ). In panel (c) we have summed panels (a) and (b) to notice that positron wavefunction effects are reinforced at the expense of the FS signatures.

The very appealing message, and the main point of this paper, is however provided by panel (d), where most of the positron wave function effects cancel out and the almost intact topology of the FS is restored.

As anticipated, the difference eliminates the contribution from the non spin polarized bands and any positron wave function effect to be ascribed to them. The cancellation of positron effects caused by all the non magnetic bands, which is obviously effective also for ferromagnetic insulators [23], is clearly of great importance in

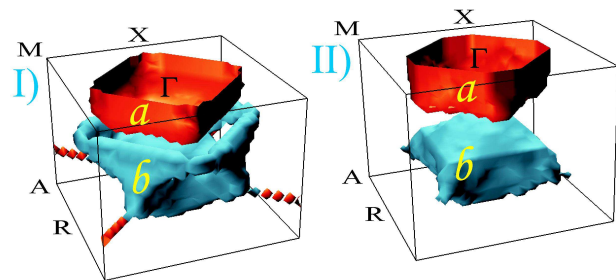


FIG. 3: Spin polarized FSs seen by 2D-ACAR experiments in  $\text{CrO}_2$ , shown in half BZ (theoretical prediction). The FSs are identified by the two isodensity surfaces (a,b) extracted from  $\rho_{LCW}^{ep, spin}(\mathbf{k})$  as described in the text. (Online color: a:orange, electronlike; b:blue, holelike). The pertaining LCW densities were produced with  $U_{xc}$  from LSDA (left, I) and GGA (right, II) [16, 17].

systems with several atoms in the unit cell and, consequently, several bands near to  $E_F$ . A similar effect can be inferred from Fig. 9 of Ref.[11]a), referring to the half metal  $\text{NiMnSb}$ . In  $\text{CrO}_2$  the visibility of the FS is further enhanced by the weakness of the positron modulation of the conduction bands. This result is consistent with the constancy of the d orbital character in the BZ for all the conduction bands, noted above.

The similarity of panel 2(d) with the theoretical occupancy (whose breaks denote the FS) makes feasible algorithms aimed at extracting the FS from isodensity surfaces of the LCW density. This task would be impossible for the data set shown in panel 2(a), where, owing to positron modulation, the amplitude of the LCW density nearby the Fermi break of a single sheet changes noticeably in the BZ. Conversely,  $\rho_{LCW}^{ep, spin}(\mathbf{k})$  presented in panel 2(d) allows to separate very clearly the two conduction bands and apply the method presented in Ref. [24] which identifies a multi-sheet FS in terms of isodensity surfaces selected at the loci of maximal amplitude variation of the LCW density. It is worth noticing that in the half metals the analysis of  $\rho_{LCW}^{ep, spin}(\mathbf{k})$  for the search of the FS manifolds is particularly suited. In fact, since the subtraction of the *insulating* LCW (down) spin density from the *conducting* LCW (up) spin density preserves the proper sign in the jumps of the occupancy due to the FS breaks, maxima of  $\rho_{LCW}^{ep, spin}(\mathbf{k})$  will correspond to maxima of the occupancy and viceversa. Fig 3 shows the resulting isodensity surfaces of  $\rho_{LCW}^{ep, spin}(\mathbf{k})$ . The similarity with the true FS shown in Fig. 1 is striking. The cancellation of positron wave function effects shows that 2D-ACAR has the power to investigate the FS predictions of LSDA and GGA, shown in Fig. 1. The difference in the FS is well revealed in the (110) plane. To establish to what extent feasible experiments can accomplish this task, in Fig. 4 we have simulated in full the output of the experiment, accord-

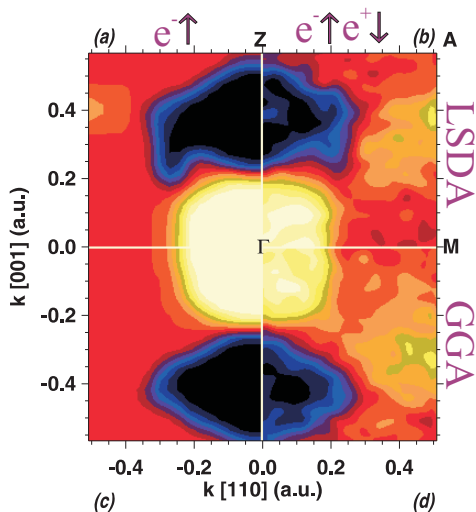


FIG. 4: (Online color.) FLAPW calculations for  $\text{CrO}_2$  in the (110) plane of the tetragonal BZ. (a) LSDA up spin occupancy convoluted with the experimental resolution; (b) LSDA simulated experimental difference spectra (inclusive of statistical noise; see text),  $\rho_{LCW\ spin}^{ep}(\mathbf{k})$ ; (c) same as (a) for GGA; (d) same as (b) for GGA.

ing to eq. 2. The steps adopted to produce Fig. 4 are, in succession: i) Calculation (adopting  $U_{xc}$  from GGA and LSDA) of  $\rho_{LCW\ par}^{ep}(\mathbf{k})$  and  $\rho_{LCW\ antipar}^{ep}(\mathbf{k})$  according to the mixing shown in eq. 2, employing the realistic positron polarization  $P_{e^+} = 0.35$ ; ii) Convolution of  $\rho_{LCW\ par}^{ep}(\mathbf{k})$  and  $\rho_{LCW\ antipar}^{ep}(\mathbf{k})$  with the experimental resolution  $R$  [25]; iii) Perturbation of the two simulated densities with statistical noise. It is assumed that the LCW density was reconstructed from 5 projections, each collecting  $5 \times 10^8$  coincidence counts, and that the spectra were symmetrized in the 3D reconstruction procedure [24]; iv) Construction of  $\rho_{LCW\ spin}^{ep}(\mathbf{k})$ .

Figure 4 shows the electronic occupancy (reflecting the FS topology) convoluted with the experimental resolution [panels (a),(c)] compared to the difference spectra resulting from steps i)-iv) [panels (b),(d)] for LSDA and GGA, respectively. Interestingly, the bulging of the LSDA holelike FS at  $\simeq (0.27, 0.20)$  a.u. [panel (a)], absent in the GGA holelike FS [panel (c)] is well reproduced by the difference  $\rho_{LCW\ spin}^{ep}(\mathbf{k})$  [panel (b)] and not present in panel (d). Obviously, to reveal the FS subtleties at stake, arrays with large number of counts are required, particularly when differences between experimental spectra are analyzed. With this caveat, we predict that a 2D-ACAR experiment should decide over this issue.

In conclusion, we have pointed out the power of the magnetic LCW procedure to eliminate large part of the modulation of the LCW density due to the non uniform positron density and reveal the FS in great detail. We have proved that this indeed happens by applying our scheme to calculate the LCW density of the half metal  $\text{CrO}_2$ . We have simulated in full the output of an experi-

ment performed with partial polarization of the positron, dictating the amount of data collection required to have appropriate signal to noise ratios. Note that the ability to include s.o. effect can be employed to corroborate 2D-ACAR measurements aimed at determining the polarization of the conduction electrons at the Fermi surface. This type of information could be of critical importance for the design of novel materials to be employed in the implementation of the future spin-based FET.

We thank Allen Mills for stimulating discussions. Work supported by CNID and project MSM 0021620834 financed by Ministry of Education of Czech Republic.

# ENEA, Via Don Fiammelli 2, 40129 Bologna, Italy

- [1] S. Berko *Proc. Int. School Phys. Enrico Fermi* (1983) ed W Brandt and A Dupasquier (Amsterdam North Holland) p64
- [2] C. K. Majumdar *Phys. Rev.* **140**, A227 (1965)
- [3] D. G. Lock, V. H. Crisp, and R. N. West, *J. Phys. F* **3**, 561 (1973)
- [4] J. H. Kaiser, R. N. West and N. Shiotani, *J. Phys. F* **16**, 1307 (1986)
- [5] E. Boronski, R. M. Nieminen, *Phys. Rev. B* **34**, 3820 (1986)
- [6] J. Ruzs, M. Biasini, A. Czopnik, *Phys. Rev. Lett.* **93**, 156405 (2004).
- [7] R.N. West, *J. Phys. Chem. Sol.* **53**, 1669, 1992
- [8] P.A. Sterne, R.H. Howell, M.J. Fluss, J.H. Kaiser et al., *J. Phys. Chem. Solids* **54**, 1231 (1993)
- [9] S. Berko and A.P.Mills, *J. Phys. (Paris) Colloq.* **32**, C1-287 (1971).
- [10] P. Genoud, A.A. Manuel, E. Walker, M. Peter, *J. Phys. Condens. Matter* **3** (23): 4201, (1991)
- [11] a) K.E.H. Hanssen and P.E. Mijnarends, *Phys. Rev. B* **34**, 5009 (1986), b) K.E.H. Hanssen, P.E. Mijnarends et al., *Phys. Rev. B* **43**, 1533(1990).
- [12] P. Sorantin and K. Schwarz, *Inorg. Chem.* **31**, 567 (1992)
- [13] I.I. Mazin, D.J.Singh, C. Ambrosch-Draxl, *Phys. Rev. B* **59**, 411 (1999).
- [14] J. Kuneš, P. Novák, P. M. Oppeneer, C. König, M. Fraune et al., *Phys. Rev. B* **65**, 165105 (2002)
- [15] A. Toropova, G. Kotliar, S.Y. Savrasov, V.S. Oudovenko, *Phys. Rev. B* **71**, 172403 (2005)
- [16] P. Hohenberg, W. Kohn, *Phys. Rev.* **136**, B864 (1964)
- [17] J.P Perdew, K. Burke and M. Ernzerhof, *Phys. Rev. Lett.* **77**, 3865 (1996)
- [18] E.Z. Zurmaev, A. Moewes, S.M. Butorin et al., *Phys. Rev. B*, **67** 155105 (2003)
- [19] J. Ruzs and M. Biasini, *Phys. Rev B*, **71**, 233103 (2005)
- [20] P. Blaha, K. Schwarz, et al. (2001) *WIEN2k*, Vienna University of Technology (ISBN 3-9501031-1-2)
- [21] D. Singh, W.E. Pickett, E.C. von Stetten and S. Berko, *Phys. Rev. B* **42**, R2696 (1990)
- [22] M. Biasini and J. Ruzs, to be published
- [23] T. Chiba, *J. Chem. Phys.* **64**, 1182 (1976); P.E. Mijnarends, R.M. Singru, *Appl. Phys.* **4**, 303, (1974)
- [24] M. Biasini, G. Ferro, G Kontrym-Sznajd and A. Czopnik, *Phys. Rev. B* **66** 075126 (2002)
- [25] The adopted value  $R = 0.0685$  a.u., corresponding to 9% of the BZ along the [100] direction, is typical of existing 2D-ACAR setups.